Argininosuccinate Synthetase Is a Functional Target for a Snake Venom Anti-hypertensive Peptide

ROLE IN ARGININE AND NITRIC OXIDE PRODUCTION*[S]

Juliano R. Guerreiro[‡§], Claudiana Lameu[‡§], Eduardo F. Oliveira[‡¶], Clécio F. Klitzke[‡], Robson L. Melo[‡],
Edlaine Linares[§], Ohara Augusto[§], Jay W. Fox[∥], Ivo Lebrun[**], Solange M. T. Serrano[‡1], and Antonio C. M. Camargo[‡2]

From the ‡Center for Applied Toxicology-CAT/CEPID, Instituto Butantan, SP 05503-900, São Paulo, Brazil, the §Departamento de Bioquímica, Instituto de Química, Universidade de São Paulo, SP 05513-970, São Paulo, Brazil, the ¶Departamento de Biologia Molecular, Universidade Federal de São Paulo, SP 04044-020, São Paulo, Brazil, the ∥Department of Microbiology, University of Virginia, Charlottesville, Virginia 22908, and the **Laboratório de Bioquímica e Biofísica, Instituto Butantan, SP 05503-900, São Paulo, Brazil

Bj-BPP-10c is a bioactive proline-rich decapeptide, part of the C-type natriuretic peptide precursor, expressed in the brain and in the venom gland of *Bothrops jararaca*. We recently showed that *Bj*-BPP-10c displays a strong, sustained anti-hypertensive effect in spontaneous hypertensive rats (SHR), without causing any effect in normotensive rats, by a pharmacological effect independent of angiotensin-converting enzyme inhibition. Therefore, we hypothesized that another mechanism should be involved in the peptide activity. Here we used affinity chromatography to search for kidney cytosolic proteins with affinity for *Bj*-BPP-10c and demonstrate that argininosuccinate synthetase (AsS) is the major protein binding to the peptide. More importantly, this interaction activates the catalytic activity of AsS in a dose-dependent manner. AsS is recognized as an important player of the citrulline-NO cycle that represents a potential limiting step in NO synthesis. Accordingly, the functional interaction of *Bj*-BPP-10c and AsS was evidenced by the following effects promoted by the peptide: (i) increase of NO metabolite production in human umbilical vein endothelial cell culture and of arginine in human embryonic kidney cells and (ii) increase of arginine plasma concentration in SHR. Moreover, α-methyl-DL-aspartic acid, a specific AsS inhibitor, significantly reduced the anti-hypertensive activity of *Bj*-BPP-10c in SHR. Taken together, these results suggest that AsS plays a role in the anti-hypertensive action of *Bj*-BPP-10c. Therefore, we propose the activation of AsS as a new mechanism for the anti-hypertensive effect of *Bj*-BPP-10c in SHR and AsS as a novel target for the therapy of hypertension-related diseases.

Inhibition of somatic angiotensin-I-converting enzyme (sACE)[3] is a widely used approach in the treatment of hypertension. The first available competitive inhibitors of sACE were the naturally occurring proline-rich oligopeptides from the venom of *Bothrops jararaca*. Clinical studies using *Bj*-BPP-9a, teprotide, the most efficient of these snake venom peptides, demonstrated the potential of sACE inhibitors as anti-hypertensive drugs (1). Highly potent inhibitors of sACE, which can be administered orally, have subsequently been developed. The first of these, captopril, was designed employing a theoretical model of the active site of sACE, based on its presumed similarity to the active site of carboxypeptidase A and also with reference to the C terminus of venom proline-rich peptides, which compete with sACE substrates (2). Since captopril reproduced all known pharmacological effects and sACE-inhibiting features of the proline-rich peptides (3), the interest to deepen the investigation of the biological properties of these naturally occurring sACE inhibitors dropped dramatically. However, we recently showed that the *Bj*-BPP-10c (<ENWPHPQIPP, where <E represents pyroglutamic acid), the most selective inhibitor of the active site at the C-domain of sACE (4), displays a strong and sustained anti-hypertensive effect in spontaneous hypertensive rats (SHR), independently of the inhibition of sACE (5). This result led us to hypothesize that, besides sACE, another molecule involved in the arterial blood pressure homeostasis could possibly be a target for *Bj*-BPP-10c. Two reasons prompted us to search the putative target in the kidney: (i) the crucial role played by the kidney in the arterial blood pressure control (6) and (ii) the selective concentration and long lasting permanence of [125]I-*Bj*-BPP-10c in the mouse kidney even when a saturating concentration of captopril was administered with the peptide (7).

[S] The on-line version of this article (available at http://www.jbc.org) contains supplemental Table 1 and Figs. 1–5.

[1] To whom correspondence may be addressed: Laboratório Especial de Toxinologia Aplicada, Instituto Butantan, Avenida Vital Brasil, 1500 CEP 05503-900, São Paulo, Brazil. Tel./Fax: 11-55-3726-1024; E-mail: solangeserrano@butantan.gov.br.

[2] To whom correspondence may be addressed: Center for Applied Toxinology, Instituto Butantan, Avenida Vital Brasil, 1500 CEP 05503-900, São Paulo, Brazil. Tel./Fax: 11-55-3726-1024; E-mail: acmcamargo@butantan.gov.br.

[3] The abbreviations used are: sACE, somatic angiotensin-I-converting enzyme; AsS, argininosuccinate synthetase; AsL, argininosuccinate lyase; NOS, nitric-oxide synthase; *Bj*-BPP-10c, *B. jararaca* bradykinin-potentiating peptide-10c; MDLA, α-methyl-DL-aspartic acid; L-Name, N[G]-nitro-L-arginine methyl ester; NO, nitric oxide; MALDI-TOF, matrix-assisted laser desorption ionization time-of-flight; SHR, spontaneous hypertensive rat(s); HUVEC, human umbilical vessel endothelial cell; HPLC, high pressure liquid chromatography; Cy3, cyanine 3; PBS, phosphate-buffered saline; MAP, mean arterial pressure; NHS, N-hydroxysulfosuccinimide.

In the present study, we identified the kidney argininosuccinate synthetase (AsS) as a putative target for *Bj*-BPP10c, and we show results demonstrating that the anti-hypertensive effect of this peptide in SHR is related to the activation of the arginine production in the kidney and of the citrulline-NO cycle in endothelial cells.

EXPERIMENTAL PROCEDURES

Animals—Experiments were performed using BALB/c mice (25–30 g), male guinea pigs (150–250 g), male Wistar rats (230–300 g), and SHR (230–300 g), which were bred at the animal care facility of Instituto Butantan (São Paulo, Brazil) and in the Instituto de Ciências Biomédicas (Universidade de São Paulo, São Paulo, Brazil). All animals were caged and handled under ethical conditions according to international rules of animals care, stated by the International Animal Welfare Recommendations, and in accordance with the Guidelines for the Use of Animals in Biochemical Research (8).

Cell Culture—Human embryonic kidney cells (HEK 293) (ATCC number CRL 1573) were propagated in Dulbecco's modified Eagle's medium supplemented with 2 mM L-glutamine, 10% heat-inactivated fetal bovine serum, and 100 mg/ml penicillin/streptomycin and were kept at 37 °C, 5% CO_2, in a humidified incubator. Cells were treated with a 0.5% trypsin solution and replicated when an adequate cell concentration had been reached. The medium was exchanged after 12 h and later every third day. Human umbilical vessel endothelial cells (HUVECs) were obtained from umbilical vessels donated by the Hospital of the University of São Paulo. Vessels were washed externally with 96% ethanol, and after a diagonal cut at the end of the vessel, a catheter was introduced into the vessel vein and attached to a three-way valve. The vein was washed with 20 ml of sterile saline, and the other end of the vessel was tied before injecting 1 ml of type IV collagenase solution (0.2 mg/ml/cm of umbilical vessel). The vessel was transferred to a Petri dish and incubated for 15 min at 37 °C. Cells of the internal side of the cord were removed by massage and transferred to a sterile tube. Bovine fetal serum was added to a final concentration of 10%, the suspension was centrifuged for 10 min at 3,000 × *g* at 4 °C, and the cell pellet was resuspended in 2 ml of complete medium (40% Medium 199, 40% Dulbecco's modified Eagle's medium, 18% bovine fetal serum, 1% L-glutamine, 1% penicillin/streptomycin). The cell suspension was transferred to a bottle previously treated with a 1% gelatin solution (30 min at 4 °C), and 5 ml of complete medium was added. The bottle was incubated at 37 °C, 5% CO_2, in a humidified incubator, and the medium was exchanged after 12 h and later every third day.

Peptide Synthesis and Labeling—*Bj*-BPP-10c was synthesized using an automatic synthesizer PSSM8 (Shimadzu Co.) by the solid phase peptide synthesis Fmoc (*N*-(9-fluorenyl)methoxycarbonyl) strategy (9). The synthetic peptide was purified by preparative reversed-phase chromatography (reversed-phase HPLC), and the purity and identity of the peptide were confirmed by MALDI-TOF mass spectrometry on an Ettan MALDI-TOF/Pro instrument (Amersham Biosciences) and by analytical reversed-phase HPLC in two different solvent systems. *Bj*-BPP-10c-Cy3 was prepared by the covalent conjugation of *Bj*-BPP-10c, synthesized with a free N-terminal amino group (ENWPHPQIPP), to the fluorescent dye cyanine 3 (Cy3) using the fluorolink Cy3-reactive dye (GE Healthcare) according to the manufacturer's instructions. *Bj*-BPP-10c-Cy3 was purified by reversed-phase HPLC and analyzed by MALDI-TOF mass spectrometry as described above.

Bj-BPP-10c Affinity Column—For preparation of a *Bj*-BPP-10c affinity column, a HiTrap NHS-activated HP column (GE Healthcare) was washed three times with 2 ml of 1 mM HCl before *Bj*-BPP-10c (5 mg in 1 ml of 0.2 M NaHCO₃, 0.5 M NaCl, pH 8.3) was added. After 30 min of incubation at room temperature, the column with the coupled peptide was inactivated with buffer A (0.5 M ethanolamine, 0.5 M NaCl, pH 8.3) and washed three times with 5 volumes of 0.2 M NaHCO₃, 0.5 M NaCl, pH 8.3, and stored at 4 °C in 50 mM Na₂HPO₄, 0.1%, NaN₃, pH 7.0. This column was named HiTrap-*Bj*-BPP-10c, and a control column was prepared by incubating the HiTrap NHS-activated HP column with buffer A (HiTrap-control).

Preparation of Mouse Kidney Cytosol—BALB/c mice were anesthetized with 0.05 ml of 10% ketamine and 2% xylazine (1:1) and submitted to intracardiac perfusion (from the left ventricle and through the right atrium) with 20 ml of 0.15 M NaCl and 0.01% sodium heparin at a flow rate of 4 ml/min. The kidneys were immediately removed and weighed, and a solution containing 10 mM Tris-HCl, 25 mM saccharose, 1 mM EDTA, and 1 mM phenylmethylsulfonyl fluoride, pH 7.5 (1 ml/g), was added. Kidneys were minced with scissors, and the tissue was homogenized (Polytron PT MR 3000; Kinematic AG), and centrifuged at 10,000 × *g* for 35 min at 4 °C. The supernatant containing the cytosolic proteins was stored at −20 °C until use.

Purification of Bj-BPP-10c Ligands by Affinity Chromatography—The HiTrap-*Bj*-BPP-10c column was equilibrated with 2 ml of 20 mM Tris-HCl buffer, pH 8.0. The mouse kidney cytosolic fraction (100 mg/ml protein) was applied to the column at a flow rate of 1 ml/min, and the column was washed with 10 ml of 20 mM Tris-HCl, pH 8.0. Proteins that bound to *Bj*-BPP-10c were eluted with 2 ml of 100 mM glycine, 0.5 M NaCl buffer, pH 3.0, or alternatively by competition with 2 ml of 20 mM Tris-HCl, pH 8.0, containing 5 mg/ml *Bj*-BPP-10c. The eluted material was dialyzed in 10 mM NH₄HCO₃, pH 8.0, for 12 h at 4 °C and concentrated to 0.1 ml final volume using a SpeedVac *c*oncentrator. Protein concentrations were determined by the Bio-Rad protein assay kit using bovine serum albumin as a standard. Samples were analyzed by electrophoresis on 12% SDS-polyacrylamide gels, as described by Laemmli (10).

Immunoblot—Following electrophoresis, proteins were electrotransferred to a nitrocellulose membrane, and immunostaining was performed according to Burnette (11), using as primary antibody a 1:500 dilution of anti-AsS antibody (BD Transduction Laboratories) and as second antibody a 1:7500 dilution of anti-mouse IgG conjugated to alkaline phosphatase (Promega). Blots were developed using AP buffer (5 M NaCl, 1 M Tris-HCl, pH 9.5, 1 M MgCl₂) with 115 mM 5-bromo-4-chloro-3-indolyl phosphate and 60 mM nitro blue tetrazolium as substrate.

Protein Identification by Mass Spectrometry—For protein identification, protein bands were excised, destained, and digested in-gel with trypsin (12). The tryptic peptide mixture

was lyophilized, dissolved in 0.1% trifluoroacetic acid, submitted to ZipTip C18 (Millipore Corp.), and spotted onto the sample plate of an Ettan MALDI-TOF/Pro mass spectrometer (GE Healthcare), mixed with the same volume of a saturated solution of α-cyano-4-hydroxycinnamic acid (Sigma) in 50% acetonitrile, 0.1% trifluoroacetic acid, and analyzed using $P_{14}R$ ((M + H)$^+$ = 1,533.8582) and angiotensin II ((M + H)$^+$ 1,046.5423) (Sigma) as external calibrants.

AsS Activity Assay—AsS activity was determined based on accumulation of the product pyrophosphate as inorganic phosphate, following cleavage with pyrophosphatase. AsS (1 μg) was added to the reaction buffer (20 mM Tris-HCl, pH 7.8, 2 mM ATP, 2 mM citrulline, 2 mM aspartate, 6 mM $MgCl_2$, 20 mM KCl, and 0.2 units of pyrophosphatase) to a final volume of 0.2 ml. Samples were incubated at 37 °C in 96-well microtiter plates, and the reactions were stopped after 30 min by the addition of an equal volume of molybdate buffer (10 mM ascorbic acid, 2.5 mM ammonium molybdate, 2% sulfuric acid). Accumulation of phosphate was determined spectrophotometrically at 650 nm, and concentration was extrapolated from a standard curve of inorganic phosphate.

Internalization of Bj-BPP-10c-Cy3 by HEK 293 and HUVEC—HEK 293 cells or HUVECs were seeded on coverslips, allowed to settle, and serum-starved overnight. Cell monolayers were treated with 1 μM *Bj*-BPP-10c-Cy3 at 37 °C for 30 min dissolved in serum-free medium. After treatment, cell monolayers were washed three times with PBS, fixed with 4% formaldehyde for 15 min, and washed with sterile water. Cells were then incubated with anti-fading reagent (Vector Laboratories) and visualized using a fluorescence microscope (Axiocam; Zeiss) and Cy3 filter sets (excitation 550 nm, emission 570 nm). Photomultiplier gain and laser power were kept constant throughout each experiment.

Quantification of Bj-BPP-10c Internalized by HEK 293 Cells and HUVECs—1 × 10^6 HUVECs and HEK 293 cells were seeded into 6-well culture plates in appropriate medium and incubated at 37 °C, 5% CO_2, in a humidified incubator for 24 h. Cells were then incubated in serum-free medium with 500 pmol of *Bj*-BPP-10c for 0.5, 1, 2, 3, and 4 h. After discarding the culture medium, cells were washed and lysed with 0.1 ml of PBS by freezing and thawing and centrifuged at 21,000 × g at 4 °C for 15 min. Supernatants were collected and kept at −80 °C (intracellular medium) until use. Liquid chromatography electrospray ionization mass spectrometric analyses were carried out on a liquid chromatography/mass spectrometry Surveyor MSQ Plus (Thermo Electron) in the positive mode. Samples (0.02 ml) were injected into an analytic column (source 5RPC ST 2.1/150; Amersham Biosciences) and eluted using a gradient of 20–100% B (B = 90% acetonitrile, 0.1% formic acid; A = 0.1% formic acid) in 20 min, at a flow rate of 0.2 ml/min. The capillary and cone potential were set to 3.1 kV and 40 V, respectively. *Bj*-BPP-10c was detected as a double-charged ion by selected ion monitoring of the 599 *m/z* (M + 2H)$^{2+}$, span 1 atomic mass unit, and dwell time 1 s. A standard calibration curve for the analyte was constructed by plotting the peak area against the amount of *Bj*-BPP-10c standard (5–1,000 pmol) spiked into 0.1 ml of cell lysates. The data were processed using Xcalibur version 1.4 software (Thermo Electron), and unknown sample

peak areas were then interpolated from the calibration curve to provide concentrations of *Bj*-BPP-10c.

Cell Viability Assay—Cell viability was tested using the Live/Dead kit (Invitrogen), which uses two fluorescent dyes, calcein AM and EthD-1 (ethidium homodimer), to stain live and dead cells simultaneously. 1 × 10^6 cells (HEK 293 and HUVEC) were cultured in serum-free medium in the presence or in the absence of 100 μM *Bj*-BPP-10c for 24 h at 37 °C in 96-well black-walled fluorescence plates (Costar). After this period, the medium was removed, and the cells were incubated with calcein AM (4 μM) and EthD-1 (2 μM) for 30 min at room temperature, and the fluorescence of green calcein (excitation 485 nm, emission 530 nm) or red EthD-1 (excitation 530 nm, emission 645 nm) was measured using the FlexStation 3 reader (Molecular Devices). Relative numbers of live and dead cells were calculated from the number of non-treated live cells and the number of dead cells (treated with 0.1–0.5% digitonin for 10 min) using the software SoftMax®Pro (Molecular Devices).

Determination of Intracellular and Extracellular Arginine Levels in HEK 293 Cells by HPLC/Amino Acid Detection Analysis—1 × 10^6 cells were cultured in serum-free medium containing 0.01–100 μM *Bj*-BPP-10c and/or 1 mM MDLA (Sigma) for 24 h at 37 °C. The culture medium was collected (extracellular medium), and the cells were washed five times with Krebs solution (118 mM NaCl, 4.7 mM KCl, 1.2 mM KH_2PO_4, 1.17 mM $MgSO_4$, 2.5 mM $CaCl_2$, 25 mM $NaHCO_3$, 5.6 mM glucose), resuspended with 0.1 ml of Krebs solution, and proteins were extracted with 0.5 ml of methanol. The mixture was centrifuged for 2 min at 10,000 × g to remove cell debris, and 0.2 ml of the supernatant (intracellular medium) was mixed with 0.8 ml of PBS. Oasis MCX SPE columns (Waters) were used without preconditioning, and all washing and elution steps were performed by vacuum suction. After sample application, the columns were consecutively washed with 1 ml of 100 mM HCl and 1 ml of methanol. Bound analytes were eluted with 1 ml of ammonia/water/methanol (10/40/50) and dried in a SpeedVac concentrator at 70 °C. The dried material was derivatized with phenylisothiocyanate for arginine determination, as previously described (13, 14). Briefly, the dried samples were directly derivatized with 0.03 ml of phenylisothiocyanate reagent (75% ethanol/water (7:1), 12.5% triethylamine, 12.5% phenylisothiocyanate). After vigorous mixing, the mixture was incubated for 10 min at room temperature, 0.17 ml of water was added, and 0.1 ml of the final mixture was injected into a C18 analytical column (250 mm, 4.6 mm, 5 μm; Merck) coupled to an HPLC apparatus (HP 1100 series). Elution was performed using a gradient of acetonitrile as described before (14). A standard chromatographic run of arginine was performed by injecting a 0.1 ml of a standard solution prepared as follows. 0.03 ml of a 2.5 mM arginine solution was mixed with 0.03 ml of the phenylisothiocyanate reagent, the mixture was incubated for 10 min at room temperature, and the volume was adjusted to 0.2 ml with water. A control chromatographic run was performed using 0.1 ml of phenylisothiocyanate reagent. The integrated peak areas were compared with that of the arginine standard to calculate the amount of arginine present in each sample.

Determination of Plasma Arginine Levels by HPLC/Amino Acid Detection Analysis—Bj-BPP-10c (71 nmol/kg) or MDLA (Sigma; 1 mmol/kg) was administered to SHR ($n = 6$) and to Wistar rats ($n = 3$) by intravenous bolus injection (0.5 ml). Blood was obtained by venipuncture and collected in Vacutainer tubes (BD Biosciences) containing heparin as anticoagulant. After centrifugation at $3,000 \times g$ for 10 min at 4 °C, plasma samples (0.2 ml) were mixed with 0.2 ml of PBS and submitted to chromatography on Oasis MCX SPE columns (15) and determination of plasmatic arginine levels by HPLC/fluorescence detection analysis as described above.

Chemiluminescence Assay for Measurement of Nitric Oxide Products—Determination of NOx (nitrate and nitrite) was performed with a chemiluminescence nitric oxide analyzer (NOA[280]; Sievers Instruments), following the procedure optimized by Feelisch *et al.* (16). Bj-BPP-10c was added in the concentration range of 0.01–100 μM to HUVECs grown in Petri dishes (1×10^6 cells), and incubation continued for 24 h in serum-free medium. Subsequently, 1 ml of medium was retrieved (extracellular medium) and treated with a concentrated solution of *N*-ethylmaleimide to give a final concentration of 10 mM. Cells were washed with PBS and lysed in radio-immune precipitation buffer (50 mM Tris, pH 7.5, 150 mM NaCl, 1% Nonidet p-40, 0.5% sodium desoxycholate, 0.1% SDS, 1 mM DTPA, and 10 mM *N*-ethylmaleimide). Cell lysates were collected and incubated on ice for 30 min and centrifuged at $21,000 \times g$ for 15 min at 4 °C. The supernatant (intracellular medium) and extracellular medium were directly injected into a vessel containing a saturated solution of vanadium(III) chloride in 1 N HCl maintained at 90 °C. Under these conditions, all nitric oxide-derived products (nitrate, nitrite, nitrosothiol, nitrosamines, and iron-nitrosyl complexes) were reduced to and compared with those of standard solutions of nitrate under the same experimental conditions (16, 17).

Analysis of the Phosphorylation Status of AsS—HEK 293 and HUVEC cell lines (1×10^6 cells) were treated with Bj-BPP-10c (0.5 μM) for 24 h in serum-free medium. Cell lysates were prepared by adding 1 ml of lysing buffer (50 mM Tris-HCl, pH 7.4, 150 mM NaCl, 1% Nonidet P-40, 1 mM EDTA), and lysates were centrifuged at $12,000 \times g$ at 4 °C for 10 min. Equal amounts of supernatant protein were incubated with Dynabeads protein G (Invitrogen) at 4 °C for 1 h for preclearing. Supernatants were then incubated with anti-phosphoserine/phosphothreonine antibody (BD Biosciences) at 4 °C for 4 h. The antibody-antigen complex was incubated with Dynabeads protein G for 1 h at 4 °C. After washing the beads three times with PBS, immuno-precipitated proteins were eluted by boiling the beads in a solution containing 62.5 mM Tris-HCl, pH 6.8, 25% glycerol, 2% SDS, and 0.01% bromphenol blue and quantified by the Bio-Rad protein assay kit using bovine serum albumin as a standard. For immunoblots, equal amounts of protein (1 μg) were separated on SDS-polyacrylamide gels, transferred onto nitrocellulose membranes, and immunostained with anti-AsS (BD Transduction Laboratories) or anti-glyceraldehyde-3-phosphate dehydrogenase (Novus Biologicals) antibodies according to Ref. 11. Anti-glyceraldehyde-3-phosphate dehydrogenase was used as a loading control.

Effect of MDLA in the Anti-hypertensive Activity of Bj-BPP-10c on the Blood Pressure of SHR and Wistar Rats—20 h before the experiment, under anesthesia with 23.5% tribromoethanol (1 ml/100 g body weight) intraperitoneally, a polyethylene catheter (PE-10 connected to PE-50) was introduced into abdominal aorta through a femoral artery for measurements of mean arterial pressure (MAP) and into a femoral vein for intravenous injection. After recovery from anesthesia, the rats were kept in individual cages with free access to water and chow until the end of the experiments. Before drug administration, the MAP was monitored for 1 h (base-line period). After this period, intravenous bolus injection of Bj-BPP-10c, MDLA, or 0.15 M NaCl in a total volume of 0.5 ml was carried out. Bj-BPP-10c (71 nmol/kg) or MDLA (1 mmol/kg) was administered to SHR ($n = 6$) and in Wistar rats ($n = 4$). MAP values were registered at 2-min intervals for the entire recording period (6 h).

Bradykinin Potentiation on Isolated Guinea Pig Ileum—Bradykinin potentiation assays on isolated guinea pig ileum were performed essentially as described previously (18). Male guinea pigs (150–250 g body weight) were fasted for 24 h before experiments. Segments of about 15 cm of the terminal ileum were removed and cleaned from surrounding tissues, and the lumens were carefully washed with Tyrode solution (137 mM NaCl, 2.7 mM KCl, 1.36 mM CaCl$_2$, 0.49 mM MgCl$_2$, 0.36 mM NaH$_2$PO$_4$, 11.9 mM NaHCO$_3$, 5.04 mM D-glucose), containing diphenyldramine (1 mg/ml) and atropine (1 mg/ml). After a resting period of 30 min, segments of 4.5 cm of the isolated ileum were mounted in a 5-ml chamber containing continuously aerated Tyrode solution at 37 °C. Isometric contractions were recorded by means of isometric transducers coupled to a recording system (Powerlab/4SP; AD Instruments), under a load of 1.0 g. Concentration-response curves for bradykinin were obtained in the absence (control) or presence of 3×10^{-6} M pure peptide. Dose-response curves were fitted through a non-linear regression, and pD$_2$ values ($-\log$EC$_{50}$) were calculated using the curve-fitting program Graphpad Prism 5.0 (GraphPad Software). Data were expressed as mean ± S.E.

Statistical Analysis—All data are presented as mean ± S.E. Student's *t* test was used to determine statistical differences. A *p* value of less than 0.01 was considered significant.

RESULTS

Identification of a Binding Partner of Bj-BPP-10c in the Cytosol of Mouse Kidney Cells—Following our hypothesis that Bj-BPP-10c might have another target protein besides sACE and our previous work showing the long lasting permanence of ^{125}I-Bj-BPP-10c in the mouse kidney when the peptide was administered concomitantly with a saturating concentration of captopril (7), we submitted a mouse kidney cytosol preparation to affinity chromatography using the HiTrap NHS-activated HP resin to which Bj-BPP-10c was immobilized by chemical conjugation. As shown in Fig. 1A, a major protein bound to the resin and was eluted with 100 mM glycine, 0.5 M NaCl, pH 3.0 (elution buffer). The same protein profile was obtained when the bound fraction was eluted by competition with 5 mM Bj-BPP-10c. Confirming the specificity of binding to Bj-BPP-10c, a similar elution profile was obtained when the cytosolic proteins were prechromatographed on a HiTrap-control col-

A

B

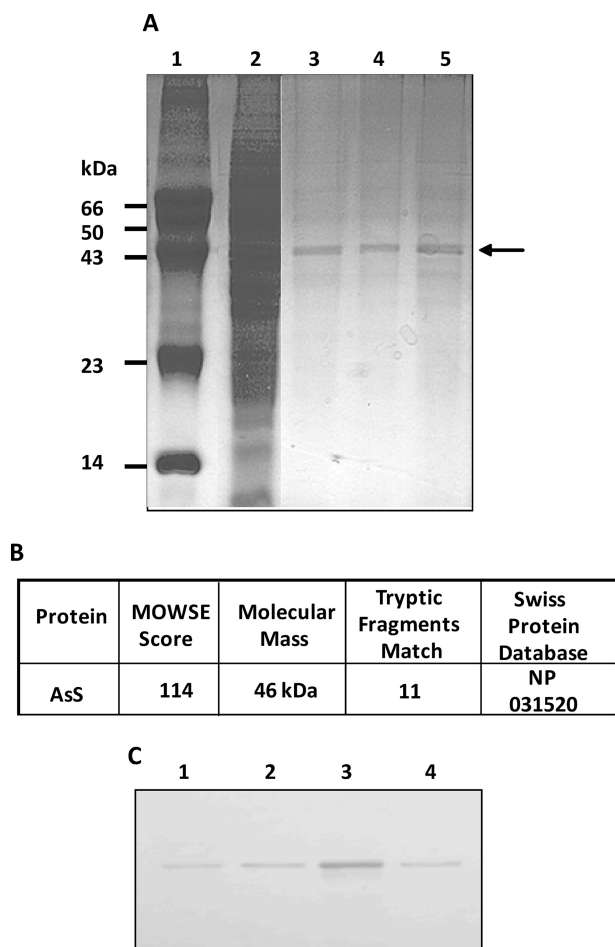| Protein	MOWSE Score	Molecular Mass	Tryptic Fragments Match	Swiss Protein Database
AsS	114	46 kDa	11	NP 031520

C

FIGURE 1. **AsS binds to *Bj*-BPP-10c.** *A*, SDS-PAGE analysis of kidney mouse cytosolic proteins submitted to HiTrap-*Bj*-BPP-10c affinity chromatography. *Lane 1*, molecular mass markers; *lane 2*, mouse kidney cytosolic proteins (50 μg); *lane 3*, protein eluted with 100 mM glycine, 0.5 M NaCl, pH 3.0 (elution buffer) (10 μg); *lane 4*, protein eluted by competition using 5 mM *Bj*-BPP-10c (10 μg); *lane 5*, protein obtained by prechromatography of the cytosolic proteins on the HiTrap-control column followed by chromatography on the HiTrap-*Bj*-BPP-10c column and eluted with elution buffer (10 μg). *B*, protein identification by mass spectrometric analysis of the band indicated by an *arrow* in *A*. *C*, immunoblot of the mouse cytosolic proteins (50 μg) and fractions obtained by affinity chromatography (1 μg). *Lanes 1–4* correspond to *lanes 2–5* of *A*.

umn followed by chromatography on the HiTrap-*Bj*-BPP-10c column and eluted with elution buffer. The 46-kDa major protein that bound to *Bj*-BPP-10c was identified by trypsin digestion and peptide mass fingerprint as AsS (EC 6.3.4.5), an enzyme that catalyzes the synthesis of argininosuccinate from citrulline and aspartate (Fig. 1*B* and supplemental Table 1). An anti-AsS antibody also recognized the 46-kDa protein in an immunoblot assay (Fig. 1*C*).

Activation of AsS Catalytic Activity by Bj-BPP-10c—In hepatocytes, in kidney proximal tubules, and in NO-producing cells, AsS catalyzes the conversion of citrulline, L-aspartate, and ATP to argininosuccinate, AMP, and pyrophosphate (19). In order to verify whether the interaction between *Bj*-BPP-10c and AsS was functional, we first tested the effect of the peptide on the catalytic activity of the enzyme. AsS obtained by *Bj*-BPP-10c affinity chromatography (1 μg, which was within the linear range of AsS activity *in vitro*) was incubated with *Bj*-BPP-10c at various concentrations. Under these conditions, *Bj*-BPP-10c

showed a dose-dependent activation of AsS activity illustrated by a bell-shaped curve (Fig. 2*A*). MDLA, a specific inhibitor of AsS (20, 21), completely abolished its enzymatic activity in the presence of *Bj*-BPP-10c (Fig. 2*A*). The contribution of individual amino acids to the AsS activation by *Bj*-BPP-10c was evaluated by the substitution of two Pro residues located in the middle of *Bj*-BPP-10c sequence and the residues of the C terminus (Ile-Pro-Pro) by Ala residues. Supplemental Fig. 1 shows that all individual substitutions partially affected the ability of *Bj*-BPP-10c to enhance AsS enzymatic activity, whereas the C-terminal Pro residues seem to be essential for the peptide engagement with AsS.

Considering that 0.5 μM *Bj*-BPP-10c caused a significant activation of AsS (Fig. 2*A*), we tested the effect of this peptide concentration on the substrate affinity of AsS for its substrates (ATP, citrulline, and aspartate). Toward this end, AsS was incubated with 0.5 μM *Bj*-BPP-10c and various concentrations of only one of the three substrates. The two other substrates were added at a fixed concentration of 2 mM, and the product formation was assayed for 30 min (Fig. 2, *B–D*). A plot of 1/velocity *versus* 1/[substrate] revealed that the affinity of AsS for ATP and citrulline was significantly increased by the peptide, since the K_m value for these substrates decreased 4.4- and 2.0-fold, respectively. In contrast, the K_m value for aspartate did not change (Fig. 2*E*). Moreover, since a decrease in the activity of AsS was observed at concentrations of *Bj*-BPP-10c above 2 μM (Fig. 2*A*), we decided to test whether a higher concentration of the peptide would affect the interaction of AsS with its substrates. Fig. 2, *B–D*, shows that plots of 1/velocity *versus* 1/[substrate] determined in the presence of 100 μM *Bj*-BPP-10c were similar to those determined in the absence of the peptide.

Internalization of Bj-BPP-10c by HUVEC and HEK 293 Cells— In order to further test the functionality of the *Bj*-BPP-10c/ AsS interaction, we tested whether the peptide could be internalized by AsS-expressing endothelial (HUVEC) and kidney (HEK 293) cells, which showed the presence of AsS by Western blot (supplemental Fig. 2). For the internalization assay, *Bj*-BPP-10c was labeled with Cy3 dye, and the labeled peptide was initially tested for its ability to activate AsS catalytic activity, which was not affected by the labeling with Cy3 (not shown). More importantly, the ability of *Bj*-BPP-10c-Cy3 to potentiate bradykinin activity on isolated guinea pig ileum was similar to that of the unlabeled peptide (supplemental Fig. 3); therefore, *Bj*-BPP-10c-Cy3 (0.5 μM) was incubated with HUVECs for 30 min at 37 °C, and the cells were submitted to fluorescence microscopy visualization. *Bj*-BPP-10c-Cy3 was detected homogenously distributed within the cell cytoplasm (Fig. 3). In a previous work, a similar internalization profile was observed when HEK 293 cells were incubated with *Bj*-BPP-10c-Cy3 (7).

In parallel, we quantified *Bj*-BPP-10c uptake by both HUVECs and HEK 293 cells by liquid chromatography/mass spectrometry. *Bj*-BPP-10c (500 pmol) was incubated with 1 × 10^6 cells for 4 h, and the intracellular medium was analyzed for the identification and quantification of *Bj*-BPP-10c. As shown in Fig. 3, *D* and *E*, up to 2 h of incubation, ~10 and 15% of the total amount of *Bj*-BPP-10c used (500 pmol) was found in the intracellular medium of HEK 293 cells and HUVECs,
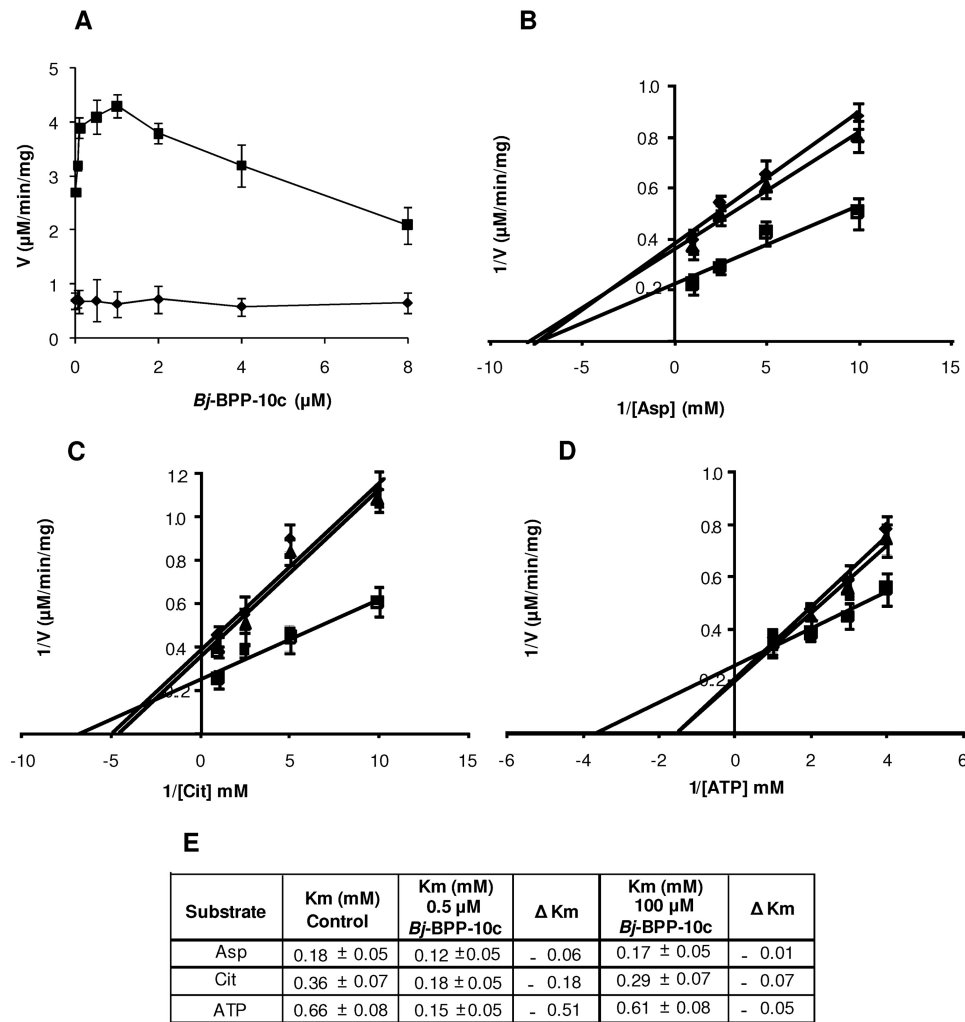
A

B

C

D

E

Substrate	Km (mM) Control	Km (mM) 0.5 μM *Bj*-BPP-10c	Δ Km	Km (mM) 100 μM *Bj*-BPP-10c	Δ Km
Asp	0.18 ± 0.05	0.12 ±0.05	− 0.06	0.17 ± 0.05	− 0.01
Cit	0.36 ± 0.07	0.18 ±0.05	− 0.18	0.29 ± 0.07	− 0.07
ATP	0.66 ± 0.08	0.15 ±0.05	− 0.51	0.61 ± 0.08	− 0.05

FIGURE 2. ***Bj*-BPP-10c enhances AsS enzymatic activity.** *A*, effect of *Bj*-BPP-10c on the enzymatic activity of 1 μg of AsS obtained by HiTrap-*Bj*-BPP-10c-affinity chromatography. *Squares*, activity in the absence of MDLA; *diamonds*, activity in the presence of 1 mM MDLA. *B–D*, effect of *Bj*-BPP-10c on the affinity of AsS for its substrates. AsS activity was measured in the absence (*triangles*) or in the presence of 0.5 μM *Bj*-BPP-10c (*squares*) or 100 μM *Bj*-BPP-10c (*diamonds*) and the indicated concentrations of only one of the three substrates (citrulline (*Cit*), Asp, or ATP) and a 2 mM concentration of the other two substrates for 30 min. Double reciprocal plots of substrate concentration *versus* reaction velocity are depicted for citrulline, Asp, and ATP. *E*, K_m values obtained in the absence and in the presence of *Bj*-BPP-10c were estimated using non-linear fitting (Graphpad Prism 5.0). Values are mean ± S.E. of 3–4 replicates.

respectively. However, at higher incubation times (2–4 h), intact *Bj*-BPP-10c was not detected inside both cell lines, suggesting that it might have been metabolized by the cells.

Bj-BPP-10c Enhances Arginine Production in HEK 293 Cells— Arginine is recognized as a conditionally essential amino acid in adults. Although numerous cell/tissues are able to synthesize arginine, it is well established that the kidney is the major site of its synthesis in humans (22). Since *Bj*-BPP-10c bound to AsS of mouse kidney cytosol (Fig. 1*A*), we decided to test the effect of the peptide in the arginine production by a kidney cell line. Therefore, HEK 293 cells were treated with increasing concentrations of *Bj*-BPP-10c (0.01–100 μM) for 24 h, and the intracellular and extracellular concentrations of arginine were determined. The intracellular and extracellular basal levels of arginine in these cells were 50 ± 4 nmol/10[6] and 9 ± 3 nmol/10[6] cells, respectively. The peptide caused a striking dose-response increase of arginine both in the intracellular and extra-

cellular media (2- and 6-fold, respectively), which peaked at 0.5–2 μM *Bj*-BPP-10c (Fig. 4*A*). However, at higher peptide concentrations (4–100 μM), a slight decrease in arginine production was observed (Fig. 4*A*). In order to check whether the enhancement of arginine production induced by *Bj*-BPP-10c was related to the activation of AsS, we tested the effect of MDLA in this assay (20, 21). The concomitant treatment of HEK 293 cells with 0.5 μM *Bj*-BPP-10c and 1.0 mM completely abolished the effect of *Bj*-BPP-10c upon arginine production (Fig. 4*B*), confirming the involvement of AsS in the observed enhancement of arginine generation by the peptide.

Bj-BPP-10c Enhances the Plasma Level of Arginine in SHR and Wistar Rats—Studies on the development of hypertension in SHR have focused on the effect of arginine, since the endogenous vasodilator NO is known to be synthesized from arginine in the endothelium of blood vessels to counteract the increases in blood pressure at the local level (23). In the current study, we determined the effect of *Bj*-BPP-10c in arginine plasma concentration in SHR and Wistar rats for 6 h. As shown Fig. 5, the administration of 71 nmol/kg *Bj*-BPP-10c increased the arginine plasma levels in SHR (from 2.2 ± 0.15 to 3.1 ± 0.25 μM) and in Wistar rats (from 0.9 ± 0.05 to 1.2 ± 0.05 μM). As observed with HEK 293 cells, when 1 mmol/kg MDLA was administered together with *Bj*-BPP-10c, no change in the arginine plasma level was observed in both SHR and Wistar rats (Fig. 5). Interestingly, after 1 h of co-infusion of peptide and inhibitor, there was a slight decrease in the arginine plasma level compared with the basal level both in SHR (from 2.2 ± 0.15 to 1.7 ± 0.2 μM) and Wistar rats (from 0.9 ± 0.05 to 0.65 ± 0.1 μM); however, after 2 h, values returned to basal level.

Bj-BPP-10c Induces NO Metabolite Production by HUVECs— Arginine is a substrate of endothelial NO synthase, which is converted to citrulline and NO in endothelial cells. Citrulline, through the reactions catalyzed by AsS and argininosuccinate lyase (AsL) may cycle to arginine, constituting an arginine-citrulline cycle (24). Considering that the production of arginine from citrulline in a tightly coupled process provides a segregated source of arginine for NO production in endothelial cells (21), an increase of AsS activity should result in an increase in the amount of NO produced. To test
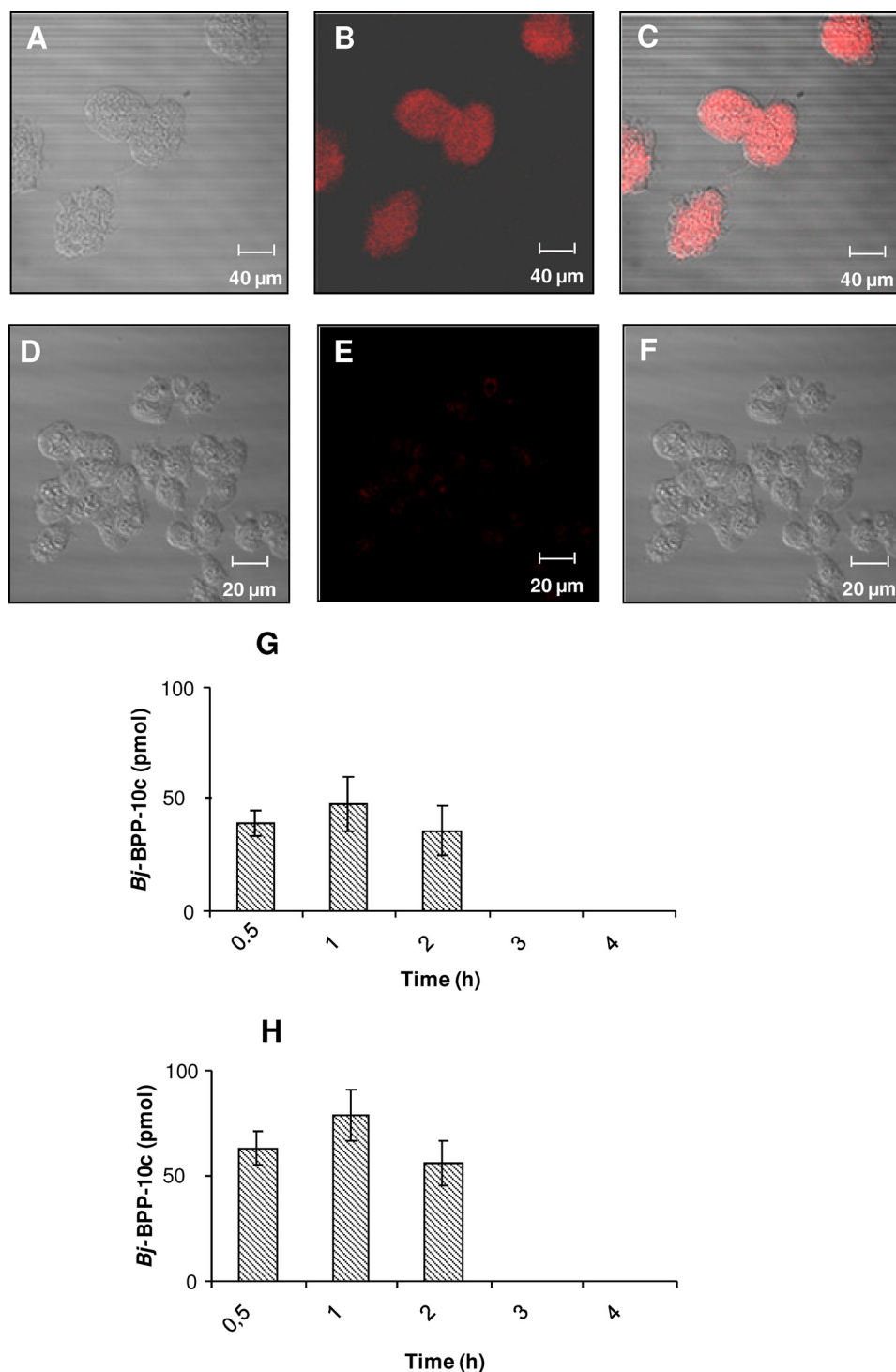
FIGURE 3. ***Bj*-BPP-10c is internalized by HUVECs.** Cells were incubated with 1 μM *Bj*-BPP-10c-Cy3 for 30 min at 37 °C and analyzed by fluorescence microscopy. Images are representative of three individual experiments. *A*, phase contrast of the HUVECs treated with *Bj*-BPP-10c-Cy3. *B*, fluorescence of *Bj*-BPP-10c-Cy3. *C*, *merged images* of *A* and *B*. The corresponding phase-contrast images of non-treated HUVECs show control cell morphology (*D–F*). *G* and *H*, quantification of *Bj*-BPP-10c internalized by HEK 293 cells (*G*) and HUVECs (*H*) by mass spectrometric analysis. *Bj*-BPP-10c amount was expressed as mean $\pm$ S.E. of four experiments.

respectively. When the cells were treated with 0.01–100 μM *Bj*-BPP-10c, the intracellular and extracellular NO metabolite concentration showed a dose-response increase (2.5- and 3.7-fold, respectively), which peaked at 0.1–2 μM *Bj*-BPP-10c (Fig. 6*A*). However, at higher peptide concentrations (4-100 μM), a slight decrease in NO metabolites production by the cells was observed (Fig. 6*A*). These results together with the observed slight decrease in arginine production by HEK 293 cells incubated with high peptide concentrations (Fig. 4*A*) prompted us to test the effect of *Bj*-BPP-10c (100 μM) upon cell viability. However, at this concentration, *Bj*-BPP-10c did not show any cytotoxic effect and did not affect the viability of HEK 293 cells and HUVECs (supplemental Fig. 4).

The concomitant treatment of HUVECs with 0.5 μM *Bj*-BPP-10c and 1 mM L-Name, a specific inhibitor of NOS, or 1.0 mM MDLA completely abolished the effect of *Bj*-BPP-10c in NO production (Fig. 6*B*), indicating the involvement of NOS and AsS in the observed increase of NO metabolite production by the peptide.

In order to explore the hypothesis that phosphorylation of AsS could be involved in the enhanced NO production observed upon the treatment of HEK 293 cells and HUVECs with *Bj*-BPP-10c, we have checked the phosphorylation status of AsS when the cells were treated for 24 h with the peptide (0.5 μM). Although AsS appeared phosphorylated, it showed the same extent of phosphorylation in control and peptide-treated cells, indicating that phosphorylation does not play a role in NO production induced by *Bj*-BPP-10c (supplemental Fig. 5).

Effect of MDLA in the Anti-hypertensive Activity of Bj-BPP-10c on the Blood Pressure of SHR and Wistar Rats—Recently, we showed that the anti-hypertensive effect of *Bj*-BPP-10c occurs in SHR but not in normotensive Wistar rats (5). In order to further explore the findings of the current study showing the activation of AsS activity by *Bj*-BPP-10c, we decided to check the effect of MDLA on the anti-hypertensive effect of the peptide in SHR and Wistar rats. Fig. 7 shows the
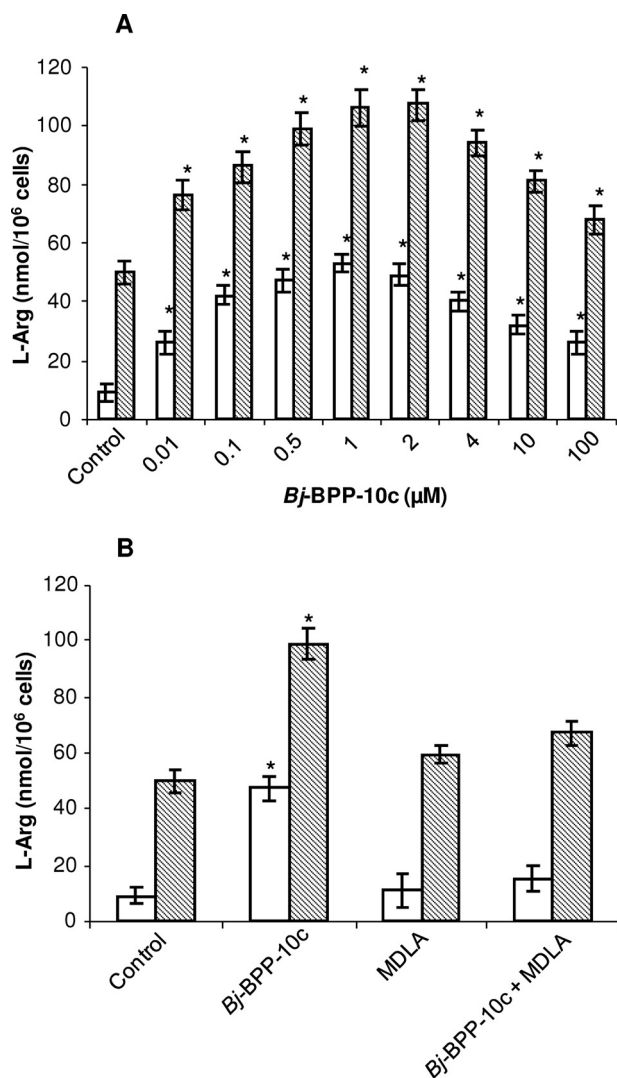
whether *Bj*-BPP-10c could stimulate the NO production by AsS activation, we determined NO metabolite concentration in intracellular and extracellular media of HUVEC culture for 24 h under treatment with *Bj*-BPP-10c. The intracellular and extracellular basal levels of NO metabolites in these cells were 1.8 $\pm$ 0.2 nmol/10^6 cells and 0.4 $\pm$ 0.05 nmol/10^6 cells,

A

B

FIGURE 4. **Bj-BPP-10c induces arginine production in HEK 293 cells.** HEK 293 cells were seeded into 6-well culture plates in appropriate medium and incubated for 24 h. Afterward, cells were incubated in serum-free medium with increased concentrations of *Bj*-BPP-10c and/or 1 mM MDLA for 24 h. The medium was collected, and the cells were lysed for determination of arginine extracellular and intracellular levels by HPLC analysis. *A*, *Bj*-BPP-10c-induced arginine production by HEK cells. *B*, effect of 1 mM MDLA in the arginine production induced by 0.5 μM *Bj*-BPP-10c. Arginine concentration was expressed as mean ± S.E. of six experiments. *Open bars*, extracellular medium; *hatched bars*, intracellular medium. *, $p < 0.01$ compared with control.
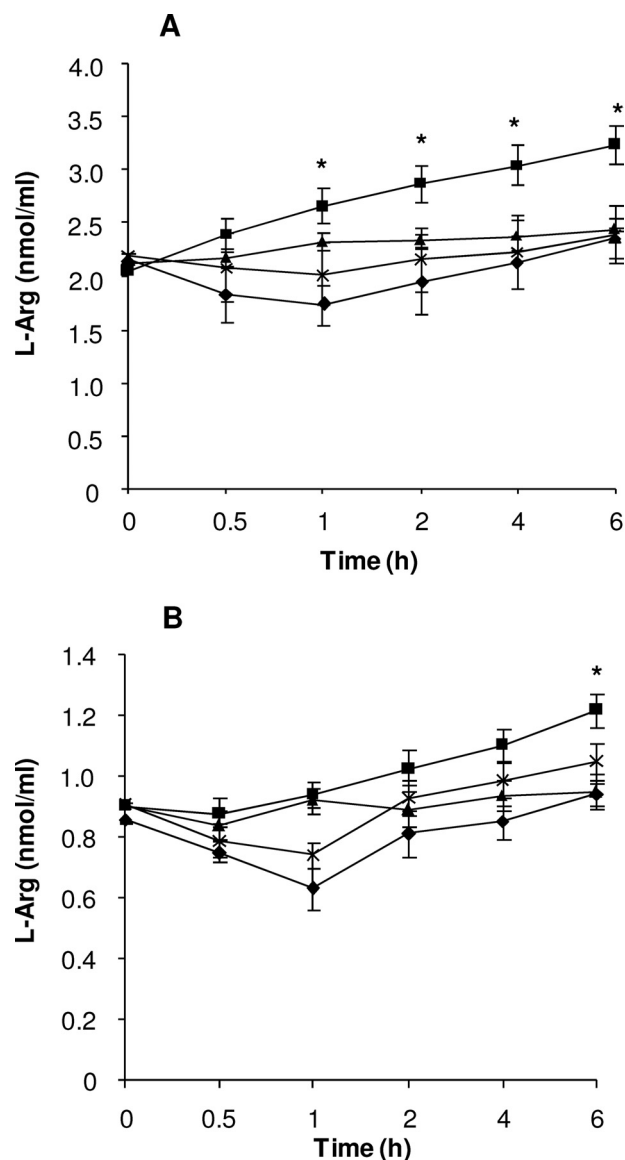
A

B

FIGURE 5. **Bj-BPP-10c enhances the plasma level of arginine.** *Bj*-BPP-10c (71 nmol/kg) or MDLA (1 mmol/kg) was administered to SHR ($n = 6$) and to Wistar rats ($n = 3$) by intravenous bolus injection (0.5 ml), and blood was obtained by venipuncture for determination of arginine level. Arginine plasma levels in SHR (*A*) or Wistar rats (*B*) after infusion of 0.15 M NaCl (*triangles*), *Bj*-BPP-10c (*squares*), MDLA (*diamonds*), or *Bj*-BPP-10c plus MDLA (×). Values are mean ± S.E. *, $p < 0.01$ compared with control.

effects on the MAP of conscious animals after the concomitant intravenous injection of 71 nmol/kg *Bj*-BPP-10c and 1 mmol/Kg MDLA. *Bj*-BPP-10c showed a significant and long lasting anti-hypertensive effect (MAP reduction from 175 ± 5 to 140 ± 5 mm Hg), which was sustained for more than 6 h in SHR (Fig. 7*A*) and no significant effect in Wistar rats (Fig. 7*B*). The administration of 1 mmol/kg MDLA alone caused a slight increase of MAP; however, its concomitant injection with *Bj*-BPP-10c impaired the anti-hypertensive effect of the peptide, pointing, for the first time, to a role of AsS in the control of blood pressure (Fig. 7*A*).

DISCUSSION

Worldwide, millions of hypertensive patients, who are treated with sACE inhibitors, have benefited from the investi-

gations by Rocha e Silva *et al.* (25) and Ferreira *et al.* (26) on the effects the venom of *B. jararaca* exerts on the cardiovascular system and on smooth muscles. Their pioneering work led to the isolation of a number of proline-rich peptides from *B. jararaca* venom that display strong inhibition of sACE. These studies were essential to reveal the pivotal role played by sACE in the regulation of the vascular tonus (27).

We focused our interest on the cardiovascular role of one specific proline-rich peptide, *Bj*-BPP-10c, mainly because it displays a strong *in vivo* bradykinin potentiation effect and is the most selective inhibitor of the active site at the C-domain of sACE (4). It is noteworthy that we showed that the inhibition of sACE was not the only mechanism involved in the anti-hypertensive effect displayed by *Bj*-BPP-10c (5). These results
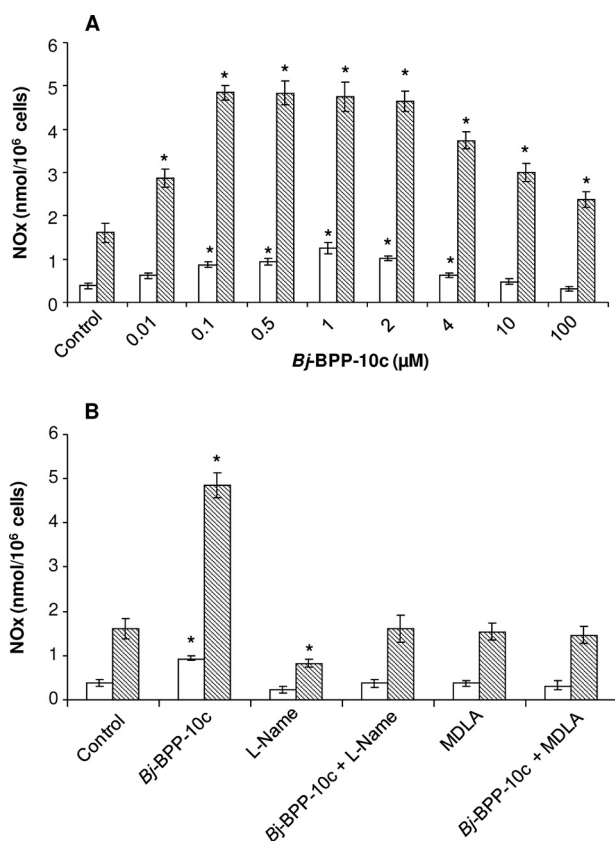
FIGURE 6. *Bj*-BPP-10c **induces NO metabolites production by HUVECs.** HUVECs were seeded into gelatin-coated Petri dishes in appropriate medium and incubated for 24 h. Afterward, cells were incubated in serum-free medium with increased concentrations of *Bj*-BPP-10c and/or 1 mᴍ MDLA and/or 1 mᴍ ʟ-Name for 24 h. The medium was collected, and the cells were lysed with radioimmune precipitation buffer to measure NO products in extracellular and intracellular media by a chemiluminescence assay. *A*, *Bj*-BPP-10c-induced NO metabolites production by HUVECs. *B*, effect of 1 mᴍ MDLA or 1 mᴍ ʟ-Name in the NO production induced by 0.5 μᴍ *Bj*-BPP-10c. NO concentration was expressed as mean ± S.E. of six experiments. *Open bars*, extracellular medium; *hatched bars*, intracellular medium. *, $p < 0.01$ compared with control.

FIGURE 7. **The anti-hypertensive effect of *Bj*-BPP-10c on blood pressure is partially impaired by MDLA.** Shown is MAP in SHR (*A*) and Wistar rats (*B*) after infusion of 0.15 ᴍ NaCl (*triangles*), 71 nmol/kg *Bj*-BPP-10c (*squares*), 1 mmol/kg MDLA (*diamonds*), or *Bj*-BPP-10c plus MDLA (×). Values are mean ± S.E. of SHR (*n* = 6) and Wistar rats (*n* = 3).

prompted us to speculate whether a different mechanism, not requiring the participation of angiotensin-II and bradykinin, could be implicated in the *in vivo* activity of *Bj*-BPP-10c. This hypothesis received support from the tissue distribution studies by Silva *et al.* (7), who showed that 40–50% of [125]I-*Bj*-BPP-10c remained in the kidneys of mice, even when a 1,000-fold higher molar concentration of captopril was administered with the peptide.

The key contribution of the present study is the identification of AsS as a novel target for *Bj*-BPP-10c. Affinity chromatography, using immobilized *Bj*-BPP-10c, associated with mass spectrometric and immunoblot analyses, allowed the identification of AsS as the main ligand for the peptide in the kidney cytosol. More importantly, we showed that *Bj*-BPP-10c promotes activation of AsS, assayed in the presence of the substrates ATP, citrulline, and aspartate.

In mammals, AsS, together with AsL, is part of the urea cycle in the liver and of the arginine-citrulline cycle, the major source of arginine and nitric oxide in renal and endothelial cells, respectively (see Fig. 2 of Ref. 19). These enzymatic processes are rate-limiting steps in both the urea- and the arginine-citrul-
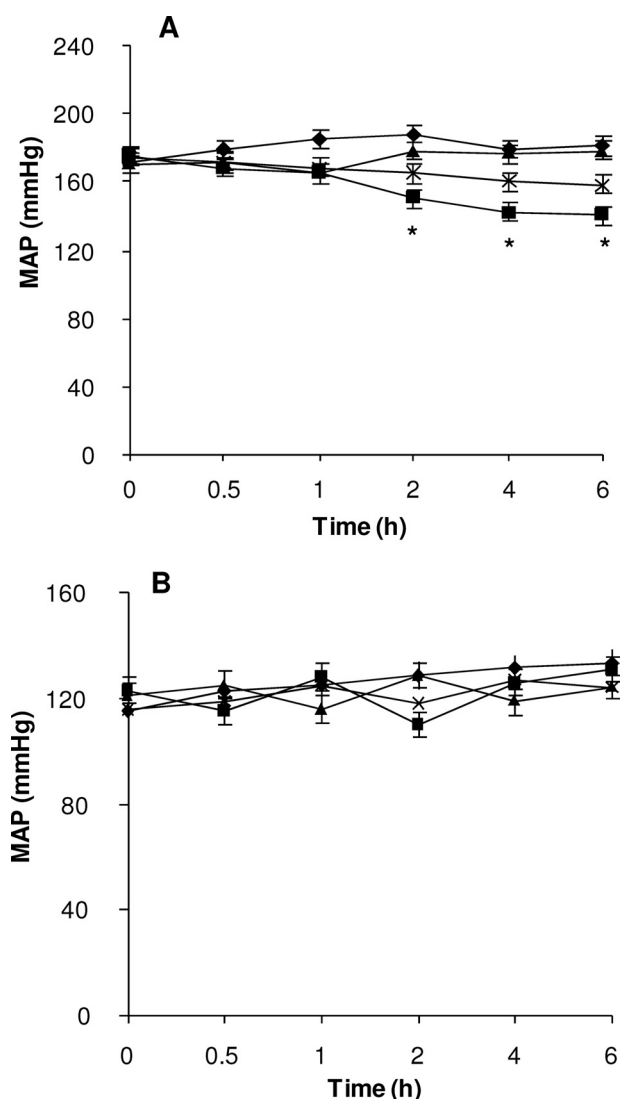
line cycles. In endothelial cells, the arginine-citrulline cycle, together with NOS, ensures the supply of NO, which plays many roles as a signaling molecule in mammalian processes, including the regulation of the vascular tonus. We hypothesized that the activation of AsS is, at any rate, part of the anti-hypertensive action of *Bj*-BPP-10c.

The influence of *Bj*-BPP-10c on the kinetics of AsS concerning its three substrates was examined by the Michaelis-Menten equation. The results indicated that at a concentration of 0.5 μᴍ, *Bj*-BPP-10c enhances the affinity of the enzyme for ATP and citrulline by 4.4- and 2.0-fold, respectively. Surprisingly, the affinity of AsS for its substrates in the presence of 100 μᴍ *Bj*-BPP-10c is similar to that determined in the absence of the peptide, suggesting that, at high concentration, the accessibility of the peptide to its own activation site may be reduced or abolished. The full understanding of the molecular mechanism of the AsS activation by *Bj*-BPP-10c should consider the state of aggregation of this enzyme. In fact, human AsS is a tetrameric

protein consisting of two identical dimers, and its overall structure is highly similar to the bacterial AsS structure. The monomer structure consists of three domains: a nucleotide-binding domain, a synthetase domain, and a C-terminal helix involved in oligomerization (28). It has been shown that *Escherichia coli* AsS undergoes a conformational change upon binding of ATP that reduces the distance between the phosphates of ATP and the citrulline molecule (29). In the case of the human enzyme, it was suggested that a small conformational change takes place upon catalysis, wherein the carbonyl oxygen atom of citrulline makes a nucleophilic attack on the α-phosphate of ATP, producing the citrullyl-AMP intermediate. Based on our finding that *Bj*-BPP-10c activates the catalytic activity of AsS, we suggest that binding of *Bj*-BPP-10c to AsS probably occurs at a site other than the substrate (ATP) and inhibitor (MDLA) binding site, promoting a conformational change of the enzyme and facilitating its interaction with ATP. This interaction could involve the binding of the peptide to each of the monomers or to one subunit of each dimer. However, the elucidation of how the interaction of *Bj*-BPP-10c and AsS results in the activation of the catalytic process must await further structural studies. Regardless of the mechanism involved in the activation of AsS by *Bj*-BPP-10c, our results show a 1.7-fold increase of AsS activity by the peptide *in vitro*, which *in vivo* probably translates into an up-regulation of the arginine-citrulline cycle in endothelial cells.

A requisite for *Bj*-BPP-10c to exert the activation of arginine biosynthesis and/or the citrulline-NO cycle is to penetrate the cells, since AsS is clearly a cytosolic enzyme (19, 30). We had previously shown that HEK 293 cells can internalize *Bj*-BPP-10c-Cy3 (7). Here we showed that *Bj*-BPP-10c-Cy3 can also penetrate HUVECs, as observed by fluorescence microscopy and by the determination of the amount of internalized peptide in both cell lines. These cells were chosen because they were originally derived from kidney and vascular endothelium, the major tissues responsible for arginine biosynthesis and NO production, respectively. We showed here that 10–15% *Bj*-BPP-10c added to the incubation medium not only penetrated the cells but also remained intact for up to 2 h. These results are not surprising, considering that *Bj*-BPP-10c is a proline-rich peptide, a feature that endows this molecule with the properties of cell-penetrating peptides, in addition to resistance to proteolysis (31).

The internalization of *Bj*-BPP-10c by HEK 293 cells was important to demonstrate the peptide's ability to activate AsS for arginine production. Accordingly, a 6-fold increase of arginine output by HEK 293 cells to the extracellular medium was detected in a concentration-dependent manner from 0.01 to 2 μM, which decreased at higher concentrations. Likewise, the intracellular arginine concentration showed a 2-fold increase induced by *Bj*-BPP-10c. The role of AsS in the increased arginine production induced by the peptide was evidenced by the clear reduction of arginine level when the cells were co-treated with the specific AsS inhibitor, MDLA.

Given that the kidney is the major site of arginine production in adult rodents, as well as in humans (19), it was not surprising to detect a significant time-dependent increase in the plasma concentration of arginine in SHR and Wistar rats after the administration of *Bj*-BPP-10c. Interestingly, the average level increase of plasma arginine was similar in SHR and normotensive Wistar rats, and in both animals this rise could be related to the activation of AsS by *Bj*-BPP-10c, since it was abolished by MDLA.

It is recognized that the impaired biosynthesis of arginine affects a number of metabolic and signaling pathways, such as the generation of a wide range of biologically active intermediates (*e.g.* nitric oxide, polyamines, creatinine, and L-amino acids) (32). Within NO-producing cells, arginine is synthesized from the NOS co-product citrulline via the sequential action of AsS and AsL. It is noteworthy that, since AsL is constitutively expressed (33), AsS serves as the rate-limiting enzyme for the continuous regeneration of arginine from citrulline, thus providing NOS with a sustained supply of substrate (34). In the present study, the dose-dependent increase of the production of NO metabolites (~3-fold) induced by *Bj*-BPP-10c in a HUVEC culture represents more clear evidence for the integrity and functionality of this peptide within the cells. The impairment of the peptide-induced production of NO metabolites by both MDLA and L-Name, a specific NOS inhibitor, confirms the activation of AsS and the involvement of NOS in the increase of NO metabolites production by HUVECs. The activation process could be regulated by dynamic AsS phosphorylation, as it has been recently demonstrated (35). However, the involvement of phosphorylation of AsS in the increase of NO production induced by *Bj*-BPP-10c in HUVECs seems unlikely, since we demonstrated that AsS does not undergo any significant change in phosphorylation degree when HUVECs are treated with the peptide.

Interestingly, it was shown here that the ability of *Bj*-BPP-10c to increase the affinity of AsS for its substrates was abolished at high peptide concentration (Fig. 2, *B–D*). Coincidentally, high concentrations of *Bj*-BPP-10c also caused a reduction in its ability to increase the arginine production in HEK 293 cells (Fig. 4) and in NO metabolite production in HUVECs (Fig. 6). This *in vitro* observation, however, may not be the dominant factor for the lower effect that higher concentrations of the peptide exerted upon the production of arginine and NO. AsS activity could be regulated, for instance, by a feedback mechanism involving NO production, since an increased production of NO may cause the *S*-nitrosylation of Cys^{132} of AsS, thus reducing the enzyme activity (36).

Finally, the striking effect of *Bj*-BPP-10c causing sustained MAP reduction in SHR contrasted with the absence of effect upon normotensive rats. More importantly, this effect was impaired by the co-administration of MDLA, indicating the participation of AsS in the control of blood pressure. The dramatically different response to *Bj*-BPP-10c found in SHR as compared with the normotensive rats is of particular interest, since the increased production of arginine up-regulates the output of NO by NO-producing cells, a phenomenon that is known to be reduced in genetically hypertensive rats (37). The importance of this system for endothelial NO production was supported by a report of two infants with a deficiency of AsL who were shown to be hypertensive (38). It has been suggested that supplemental arginine causes an increase in NO production (39, 40). This effect is described as the "arginine paradox,"

a term that has been used to refer to situations in which exogenous arginine administration seems to improve NOS activity even when arginine is available in excess (41). This phenomenon has recently been analyzed *in vivo* using a rat mesentery and small intestine microcirculatory preparation, which showed that increased bioavailability of arginine causes a significant increase in NO production throughout the microcirculation, providing direct *in vivo* evidence for the arginine paradox (42). Interestingly, our study revealed that although *Bj*-BPP-10c induced an increase of arginine plasma level in both normotensive and spontaneously hypertensive rats, the MAP was only reduced in the latter. The explanation for this fact might be related to the source of arginine, which, in the case of the *Bj*-BPP-10c-treated animals, resulted from a selected stimulation of the citrulline-arginine cycle in tissues and/or cell compartments. Recent studies support the hypothesis that the system for the recycling of citrulline to arginine utilized for NO production is composed by the recycling enzymes, AsS and AsL, which co-localize with NOS in caveolae of the plasma membrane (43). Thus, it is possible that the activity of caveolar AsS of endothelial cells is lower in SHR as compared with the normotensive rats, thus providing less arginine for NO production. This alleged dysfunction of caveolar AsS activity in SHR could be specifically corrected by AsS activation, thus providing more arginine to NOS and consequently reducing the arterial blood pressure of these animals. Nevertheless, the decreased MAP induced by the treatment of SHR with *Bj*-BPP-10c may not be directly related to the concomitant increased plasma arginine levels detected in these animals. On the other hand, the excess of NO production could be controlled by reducing the activity of AsS. It has been reported that the expression of the AsS gene was decreased in the onset of hypertension of SHR (44).

The *in vivo* increase of plasma arginine level in rats promoted by *Bj*-BPP-10c and the impairment of its anti-hypertensive effect upon SHR by MDLA suggest the functional interaction of *Bj*-BPP-10c and AsS in these events *in vivo*. Taken together, the results obtained with the snake venom proline-rich oligopeptide, *Bj*-BPP10c, provided evidence suggesting that AsS might be included among the therapeutic targets for modulation of blood pressure. Interestingly, a number of snake toxins have a counterpart in endogenous molecules of vertebrates (27, 45). In fact, the genetic origin and expression of the precursor of the proline-rich oligopeptides in *B. jararaca* tissues suggested that these peptides are part of the endocrine molecular machinery of the animal, since they are part of the precursor of the C-type natriuretic peptide expressed in the neuroendocrine region of the animal brain (46). In line with the ongoing trend of toxin-inspired drug development (47), we believe that *Bj*-BPP-10c could be considered as a lead molecule to develop therapeutic agents for the treatment of various diseases based on NO deficiency as cause or effect.

REFERENCES

1. Gavras, H., Brunner, H. R., Laragh, J. H., Sealey, J. E., Gavras, I., and Vukovich, R. A. (1974) *N. Engl. J. Med.* **291,** 817– 821
2. Ondetti, M. A., Rubin, B., and Cushman, D. W. (1977) *Science* **196,** 441–444
3. Ng, K. K., and Vane, J. R. (1970) *Nature* **225,** 1142–1144
4. Cotton, J., Hayashi, M. A., Cuniasse, P., Vazeux, G., Ianzer, D., De Camargo, A. C., and Dive, V. (2002) *Biochemistry* **41,** 6065– 6071
5. Ianzer, D., Santos, R. A., Etelvino, G. M., Xavier, C. H., de Almeida Santos, J., Mendes, E. P., Machado, L. T., Prezoto, B. C., Dive, V., and de Camargo, A. C. (2007) *J. Pharmacol. Exp. Ther.* **322,** 795– 805
6. Ram, C. V. (2008) Curr. *Hypertens. Rep.* **10,** 345–348
7. Silva, C. A., Portaro, F. C., Fernandes, B. L., Ianzer, D. A., Guerreiro, J. R., Gomes, C. L., Konno, K., Serrano, S. M., Nascimento, N., and Camargo, A. C. (2008) *Toxicon* **51,** 515–523
8. Giles, A. R. (1987) *Thromb. Haemost.* **58,** 1078–1084
9. Atherton, E., and Sheppard, R. C. (1989) *Solid Phase Peptide Synthesis-A Practical Approach*, ILR Press, Oxford
10. Laemmli, U. K. (1970) *Nature* **227,** 680–685
11. Burnette, W. N. (1981) *Anal. Biochem.* **112,** 195–203
12. Hanna, S. L., Sherman, N. E., Kinter, M. T., and Goldberg, J. B. (2000) *Microbiology* **146,** 2495–2508
13. Heinrikson, R. L., and Meredith, S. C. (1984) *Anal. Biochem.* **136,** 65–74
14. Ebert, R. F. (1986) *Anal. Biochem.* **154,** 431–435
15. Teerlink, T., Nijveldt, R. J., de Jong, S., and van Leeuwen, P. A. (2002) *Anal. Biochem.* **303,** 131–137
16. Feelisch, M., Rassaf, T., Mnaimneh, S., Singh, N., Bryan, N. S., Jourd'Heuil, D., and Kelm, M. (2002) *FASEB J.* **16,** 1775–1785
17. Linares, E., Giorgio, S., and Augusto, O. (2008) *Free Radic. Biol. Med.* **44,** 1668–1676
18. Gomes, C. L., Konno, K., Conceição, I. M., Ianzer, D., Yamanouye, N., Prezoto, B. C., Assakura, M. T., Rádis-Baptista, G., Yamane, T., Santos, R. A., de Camargo, A. C., and Hayashi, M. A. (2007) *Biochem. Pharmacol.* **74,** 1350–1360
19. Husson, A., Brasse-Lagnel, C., Fairand, A., Renouf, S., and Lavoinne, A. (2003) *Eur. J. Biochem.* **270,** 1887–1899
20. Shen, L. J., Beloussow, K., and Shen, W. C. (2005) *Biochem. Pharmacol.* **69,** 97–104
21. Flam, B. R., Eichler, D. C., and Solomonson, L. P (2007) *Nitric Oxide* **17,** 115–121
22. Morris, S. M., Jr. (2004) *J. Nutr.* **134,** 2743S–2747S
23. Jones, M. R. (1988) *J. Nutr.* **118,** 579–587
24. Hattori, Y., Campbell, E. B., and Gross, S. S. (1994) *J. Biol. Chem.* **269,** 9405–9408
25. Rocha e Silva, M., Beraldo, W. T., and Rosenfeld, G. (1949) *Am. J. Physiol.* **156,** 261–273
26. Ferreira, S. H., Bartelt, D. C., and Greene, L. J. (1970) *Biochemistry* **9,** 2583–2593
27. Hayashi, M. A., and Camargo, A. C. M. (2005) *Toxicon* **45,** 1163–1170
28. Karlberg, T., Collins, R., van den Berg, S., Flores, A., Hammarström, M., Högbom, M., Holmberg-Schiavone, L. H., and Uppenberg, J. (2008) *Acta Crystallogr. D Biol. Crystallogr.* **64,** 279–286
29. Lemke, C. T., and Howell, P. L. (2002) *J. Biol. Chem.* **277,** 13074–13081
30. Dhanakoti, S. N., Brosnan, M. E., Herzberg, G. R., and Brosnan, J. T. (1992) *Biochem. J.* **282,** 369–375
31. Pujals, S., and Giralt, E. (2008) *Adv. Drug Deliv. Rev.* **60,** 473–484
32. Wu, G., and Morris, S. M., Jr. (1998) *Biochem. J.* **336,** 1–17
33. Xie, L., and Gross, S. S. (1997) *J. Biol. Chem.* **272,** 16624–16630
34. Goodwin, B. L., Solomonson, L. P., and Eichler, D. C. (2004) *J. Biol. Chem.* **279,** 18353–18360
35. Corbin, K. D., Pendleton, L. C., Solomonson, L. P., and Eichler, D. C. (2008) *Biochem. Biophys. Res. Commun.* **377,** 1042–1046
36. Hao, G., Xie, L., and Gross, S. S. (2004) *J. Biol. Chem.* **270,** 36192–36200
37. Hasegawa, T., Takagi, S., Nishimaki, K., Morita, K., and Nakajima, S. (1992) *Biochem. Int.* **26,** 653–658
38. Fakler, C. R., Kaftan, H. A., and Nelin, L. D. (1995) *Acta Paediatr.* **84,** 460–462

39. Taylor, P. D., and Poston, L. (1994) *Br. J. Pharmacol.* **113,** 801–808
40. Lee, Y., Yang, J., Rudich, S. M., Schreiner, R. J., and Meyerhoff, M. E. (2004) *Anal. Chem.* **76,** 545–551
41. Kurz, S., and Harrison, D. G. (1997) *J. Clin. Invest.* **99,** 369–370
42. Vukosavljevic, N., Jaron, D., Barbee, K. A., and Buerk, D. G. (2006) *Microvasc. Res.* **71,** 48–54
43. Solomonson, L. P., Flam, B. R., Pendleton, L. C., Goodwin, B. L., and Eichler, D. C. (2003) *J. Exp. Biol.* **206,** 2083–2087
44. Koeners, M. P., van Faassen, E. E., Wesseling, S., de Sain-van der Velden, M., Koomans, H. A., Braam, B., and Joles, J. A. (2007) *Hypertension* **50,** 1077–1084
45. Ménez, A. (1998) *Toxicon* **36,** 1557–1572
46. Hayashi, M. A., Murbach, A. F., Ianzer, D., Portaro, F. C., Prezoto, B. C., Fernandes, B. L., Silveira, P. F., Silva, C. A., Pires, R. S., Britto, L. R., Dive, V., and Camargo, A. C. (2003) *J. Neurochem.* **85,** 969–977
47. Fox, J. W., and Serrano, S. M. (2007) *Curr. Pharm. Des.* **13,** 2927–2934